Title

INTERNAL NUCLEAR MOMENTUM AND COHERENT RECOIL OF CLUSTERS AS MECHANISMS FOR SUBTHRESHOLD ANTI-PROTON PRODUCTION IN P-NUCLEUS COLLISIONS

Authors

Shor, A.
Ganezer, K.
Perez-Mendez, V.

Publication Date

1984-07-01

LBL-17067
Preprint

Lawrence Berkeley Laboratory
UNIVERSITY OF CALIFORNIA

Submitted to Physical Review C

INTERNAL NUCLEAR MOMENTUM AND COHERENT RECOIL OF CLUSTERS AS MECHANISMS FOR SUBTHRESHOLD ANTI-PROTON PRODUCTION IN P-NUCLEUS COLLISIONS

A. Shor, K. Ganezer, and V. Perez-Mendez

July 1984

Prepared for the U.S. Department of Energy under Contract DE-AC03-76SF00098

Internal Nuclear Momentum and Coherent Recoil of Clusters as Mechanisms for Subthreshold Anti-Proton Production in P-Nucleus Collisions

A. Shor, K. Ganezer, V. Perez-Mendez
Physics Department, University of California, Los Angeles, CA
and
Lawrence Berkeley Laboratory, University of California, Berkeley, CA

Abstract

We investigate subthreshold anti-proton production in p-nucleus collisions in terms of two different production mechanisms. Calculations which consider the kinematical aspects of individual nucleon-nucleon collisions with the inclusion of internal nuclear momentum to enable subthreshold production are done. An internal nuclear momentum distribution extracted from proton production at 180° provides an excellent fit to the data on subthreshold anti-proton production. A good fit is also obtained if coherent recoil of multi-nucleon (multi-quark) clusters--rather than the high momentum components--are included in the calculations. Implications for the existence of multi-quark bags in nuclei are discussed.

Reactions in p-nucleus collisions not kinematically accessible in p-p collisions are studied for the information they contain on high momentum components and clustering within the nucleus. Recent data on proton production at 180° in p-nucleus[1,2] and nucleus-nucleus[1] collisions exhibit limiting behavior which appears to reflect on the internal nuclear momentum as discussed below. Theoretical models[3,4] which consider the backward protons to be a result of spectator recoil following the breakup of a correlated pair suggest that these protons carry direct information on the internal momentum distribution. It is not clear, however, to what extent effects such as quasi-elastic scattering,[5,6] nuclear cascading, final state interaction,[7] alter the information. Another feature of internal nuclear momentum is the possibility of subthreshold particle production, i.e., creation of particles at bombarding energies below the threshold required for their production in p-p collisions. The ability to account for the energy dependence of threshold particle production in p-nucleus collisions can serve as a corroboration of the models of internal momentum distributions extracted from data on backward proton production.

Subthreshold particle production in p-nucleus collisions may also occur as a result of collisions which involve clusters within the nucleus, which interact coherently. This possibility is especially intriguing in light of current speculation on the existence of multi-quark bags in nuclei.[8,9,10] Recent experimental results from deep inelastic scattering (DIS) of muons[11] and electrons[12] show differences in the structure function for ^{56}Fe as compared to.^{2}D These differences in the structure functions of nucleons embedded inside of nuclei cannot be attributed to Fermi momenta.[13] Although a variety of explanations for this effect have been advanced,[13] a very appealing suggestion is that of multi-quark clustering inside of nuclei. Collisions with multi-nucleon clusters, in particular those involving multi-quark bags, would provide an alternative mechanism for the subthreshold production of particles. Experimental data on subthreshold production would, therefore, pose an additional constraint on models for multi-quark clustering inside of nuclei.

In this paper, we investigate these two mechanisms for subthreshold production by a comparison with experimental data on subthreshold anti-proton production in p-nucleus collisions. We employ a simple model which emphasizes the kinematical aspects of nucleon-nucleon interactions with the inclusion of internal nuclear momentum or of coherent interactions with clusters. For the internal nuclear momentum distribution, we utilize a double-Gaussian parameterization extracted from data on proton production at 180°. For the cluster model we consider coherent interactions with 2-nucleon (6-quark) and 3-nucleon (9-quark) clusters.

Experimental measurements on subthreshold anti-proton production have been made by Dorfan et al.[15] The experimental data consist of measurements at 0° of $\overline{P}/\pi^-$ ratios in p+Cu collisions for bombarding energies ranging from 2.88 up to 6.1 GeV. The measured $\overline{P}/\pi^-$ ratios span more than six decades over this energy range. Previous attempts to fit the $\overline{P}$ yields either assumed constant π^- yields [16,17] or relied on a model to calculate these yields.[18] We have determined the anti-proton differential cross sections by multiplying the $\overline{P}/\pi^-$ ratios by π^- differential cross sections measured in p+Cu collisions.[19,20] Linear interpolation of the π^- data were made to correspond to the momenta and the bombarding energies at which the anti-protons were measured. The values we extract for the anti-proton differential cross sections using the interpolated π^- data are listed in Table 1. We estimate a 20 % error for the interpolation of the π^- differential cross sections although this is not included in the error bars for the $\overline{P}$ yields.

A large amount of data on backward yields of protons in p-nucleus collisions has been accumulating.[1,2,21,22] This phenomenon appears to be a consequence of internal nuclear momenta and correlations, although the exact process is uncertain. T. Yukawa and S. Furui [3] have shown that for proton production at 180° in p-deuterium collisions, the primary mechanism involves recoil of the spectator nucleon. They argue that the mechanism of spectator recoil following the breakup of a correlated pair must also be the dominant process in proton collision with heavier nuclei. A consequence of this mechanism is a limiting behavior at sufficiently high bombarding energy in which the shape of the backward proton distribution becomes independent of projectile energy or of target size. Their calculations imply also that at large enough bombarding energies, the proton momentum distribution at 180° becomes directly proportional to the internal momentum of the proton prior to the breakup of the correlated pair.

Geaga et al.[1] have performed a systematic study of proton production at 180° in p-nucleus and nucleus-nucleus collisions. They find a limiting behavior for bombarding energies above 1-2 GeV/nucleon. The shape of the momentum distributions for 180°

protons with momenta above 300-400 MeV/c is fitted very well with a Gaussian with a dispersion σ_2 which approaches a value of 220±10 MeV/c. They also find that the shape is almost independent of the target size or of the projectile. From this they conclude that the data provides direct information on the nuclear wavefunction.

For our calculations we assume that the double Gaussian parameterization discussed by Geaga et al. is an adequate representation of the internal nuclear momentum distribution. This distribution is given by

$$f(p)d^3\vec{p} = \left[\frac{A_1}{(\sigma_1)^3} e^{\frac{1}{2}(\frac{p}{\sigma_1})^2} + \frac{A_2}{(\sigma_2)^3} e^{-\frac{1}{2}(\frac{p}{\sigma_2})^2}\right] d^3\vec{p} \tag{1}$$

where $\int f(p)d^3\vec{p} = A =$ the total number of nucleons in the nucleus. The first term on the right hand side of Equation 1 represents the momentum distribution corresponding to a Fermi gas. The value for the Fermi momentum for ^{63}Cu within the Fermi gas model was inferred to be about 257 MeV/c from electron scattering experiments. This corresponds to a dispersion σ_1 of 115 MeV/c. (This dispersion corresponds to the RMS value of the momentum distribution projected onto one dimension.) The second term on the right hand side of Equation 1 represents the momentum components due to correlations within the nucleus. The dispersion σ_1 for the second term is taken to be 220 MeV/c which was found by Geaga et al. to be the limiting value for the distribution of protons produced at 180°. The relative normalization A_2/A_1 of the second Gaussian term as compared to the first is extracted from the ^{12}C data of Geaga et al. with the assumption of $A^{1/3}$ scaling for this ratio. The value of A_2/A_1 extrapolated for ^{63}Cu nucleus is then 0.102.

The calculations we have made for subthreshold anti-proton production also employ the double-Gaussian parameterization for the internal nuclear momentum of the target nucleons. A Monte-Carlo program was used to generate the magnitude and orientation of the internal momenta. The calculations are in the framework of the impulse approximation. This approximation is justified at bombarding energies of several GeV where the de-Broglie wavelength of the incoming proton is approximately 0.2 fm. The struck nucleon is assumed to be off the mass shell and to contribute only momentum but not energy to the collision. The invariant energy squared is taken to be

$$W = (\sqrt{\vec{p}_p^2 + M^2} + E_T)^2 - (\vec{p}_p + \vec{p}_T)^2 \qquad (2)$$

where $\vec{p}_p$ is the momentum of the bombarding proton, and $\vec{p}_T$ is the internal momentum of the struck nucleon for which the energy is given by

$$E_T = M_A - \sqrt{M_{A-1}^2 + \vec{p}_T^2} \qquad (3)$$

(i.e. the recoiling nucleus is on shell). Binding effects are assumed to be negligible. The anti-proton yield is taken to be proportional to the available phase space with the transition matrix element assumed to be constant. Calculations were made for the $\bar{p}$ differential cross sections at the measured laboratory momenta.

A fit was made to the anti-proton differential cross sections with the parameters for the double-Gaussian distribution extracted from Moniz et al. and from Geaga et al. for ^{63}Cu. Calculations were performed for each bombarding energy and secondary momentum at which the anti-proton yields were measured. The only variable parameter was the magnitude of the transition matrix element for $\overline{P}$ production which was varied in order to minimize the χ^2 for the calculations fitted to the data. A value for χ^2 of 17.7 was obtained for 15 degrees of freedom. The results of the fit are listed in Table 1. These results are shown in Figures 1 and 2, with smooth curves connecting points at which the calculations were made to guide the eye. The data points in Figure 1 represent the antiproton differential cross sections for the highest momentum measured.

A parameterization with several Gaussians has in fact been used by several authors as a representation of the internal momentum distributions in nuclei.[24,25] We have extended the above calculations for $\overline{P}$ production for various values of σ_2 and the relative amplitude A_2/A_1 between the second and the first Gaussians. The value for σ_1 was held fixed at 115 MeV/c. The χ^2 contours for the anti-proton data as a function of

σ_2 and A_2/A_1 are shown in Figure 3. The cross mark indicates the values for σ_2 and A_2/A_1 extracted from Geaga et al. for ^{63}Cu. These calculations indicate that a double-Gaussian distribution for the internal nuclear momentum can account very well for subthreshold anti-proton production, with the optimum parameters very close to those obtained from the distribution of protons ejected at 180° as measured by Geaga et al.

We have also performed similar calculations for $\overline{P}$ production in collisions involving multi-nucleon clusters which interact coherently-- with nucleons and clusters having only the conventional Fermi momentum. Collisions involving the coherent recoil of a cluster would allow for more of the incoming energy to be transferred to excitational energy, rather than to translational energy. "Universality" is assumed for anti-proton production, i.e. the $\overline{P}$ yield depends only on the available energy in the c.m. and not on the type of particles participating in the collisions. The assumption of universality has been effectively used in calculations involving the coherent tube model.[19,27,28] Clusters, as well as nucleons, are given a Fermi momentum distribution corresponding to the first Gaussian term in Equation 1. As with the previous calculation, the energy of the struck nucleon (or cluster) is such that the recoiling nucleus is on the mass shell.

A least χ^2 fit to the $\overline{P}$ data was made assuming coherent recoil of 2-nucleon and 3-nucleon clusters. The variable parameters were the fraction of the collisions which involved coherent scattering with 2-nucleon clusters and 3-nucleon clusters, as well as the transition matrix element for P production. A χ^2 of 10 for 13 degrees of freedom was obtained (Figure 4). The fraction of coherent interactions with 2-nucleon and 3-nucleon clusters necessary for fitting the $\overline{P}$ data was 0.003 and 0.00045 respectively.

This calculation for the contribution of coherent cluster recoil to subthreshold $\overline{P}$ production can also serve as an estimate of an upper limit for multi-quark bags existing in nuclei. Within the context of the above mentioned constraints, most notably the assumption of universality, the occurrence of six and nine quark bags in nuclei needed to account for subthreshold $\overline{P}$ production (assuming no high momentum components) is rather small. The result to the fit of the $\overline{P}$ data implies a level of 0.003 for 6-quark bags and 0.00045 for 9-quark bags in nuclei. This is to be contrasted with the levels required by theoretical models of multi-quark bags in nuclei, used to explain the discrepancies in the structure function of ^{56}Fe and of ^{2}D. To account for these differences, Vary and Pirner[9] had to assume levels of 0.15 for 6-quark bags and 0.015 for 9-quark bags in ^{56}Fe. Carlson and Havens [9] were able to account qualitatively for these effect by assuming a 0.3 level for 6-quark bags in nuclei. Calculations for $\overline{P}$ production containing these parameterizations for the levels of multi-quark bags in nuclei, shown in Figure 4 (with arbitrary normalization), overpredict the $\overline{P}$ production at low bombarding energies.

We conclude that the double-gaussian parameterization for the internal nuclear momentum, employed by Geaga et al. to fit backward production of protons, also provides an excellent fit to subthreshold anti-proton production in p-nucleus collisions. A good fit is also obtained if coherent recoil of multi-nucleon (multi-quark) clusters, rather than high nucleon momentum, is assumed. Given the assumption of universality, the fraction of clusters required for subthreshold $\overline{P}$ production is rather small. This places a serious constraint on models involving multi-quark bags that have been advanced to account for distortion of structure functions in DIS of leptons on nuclei.

This work was supported by the Director, Office of Energy Research, Office of High Energy and Nuclear Physics, Division of High Energy Physics of the U. S. Department of Energy under contracts DC-AC03-76SF00098 and DE-AC03-76SF00515.

References

1. J. V. Geaga et al. Phys. Rev. Lett. 45, 1993 (1980).
2. S. Frankel et al. Phys. Rev. Lett. 36, 642 (1976).
3. T. Yukawa and S. Furui, Phys. Rev. C20, 2316 (1979).
4. L. Frankfurt and M. Strikman, Phys. Lett. 83B, 407 (1979).
5. S. Frankel, Phys. Rev. Lett. 38, 1338 (1977).
6. S. Gurvitz, Phys. Rev. Lett. 47, 560, (1981).
7. R. Amado and R. Woloshyn, Phys. Lett. 69B, 400 (1977).
8. R. Jaffe, Phys. Rev. Lett. 50, 228 (1983).
9. H. Pirner and J. Vary, Phys. Rev. Lett. 46, 1376 (1981) and J. Vary, invited talk, conference on Quark Matter, Brookhaven National Laboratory (1983).
10. C. Carlson and T. Havens, Phys. Rev. Lett. 51, 261 (1983).
11. J. Aubert et al. (European Muon Collaboration) Phys. Rev. Lett. 123B, 275 (1983).
12. A. Bodek et al. Phys. Rev. Lett. 50, 1431 (1983).
13. A. Bodek and J. Ritchie, Phys. Rev. D23, 1070.
14. See references in A. Bodek et al. Phys. Rev. Lett. 51, 534 (1983).
15. D. Dorfan et al. Phys. Rev. Lett. 14, 995 (1965).
16. D. Dorfan, thesis, Columbia University, Nevis report number Nevis-159 (unpublished).
17. S. Frankel and W. Frati, Phys. Rev. C16, 1499 (1977).
18. J. Vary et al. Phys. Rev. C20, 715 (1979).
19. J. Papp, thesis, University of California, Berkeley, LBL-3633, 1975 (unpublished).
20. L. Barabash et al. Sov. J. Nucl. Phys. 24, 188 (1976).

21. Y. Bayukov, Phys. Rev. C20, 764 (1979).

22. A. Baldin et al.

23. E. Moniz et al. Phys. Rev. Lett. 26, 445 (1971).

24. O. Bohigas and S. Stringari, Phys. Lett. 95B, 9 (1980).

25. J. Zabolitzky and W. Ey, Phys. Lett. 76B, 527 (1978).

26. M. Sandel et al. Phys. Rev. C20, 744 (1979).

27. G. Berlad et al. Phys. Rev. D13, 161 (1976).

Figure Captions

Figs. 1 and 2. $P + Cu \to \overline{P} + X$

Experimental data extracted from Dorfan et al. (see text). Solid line represents calculations containing double- Gaussian distribution for the internal nuclear momentum. Parameters for the distribution are taken from Moniz et al. for the first Gaussian and from Geaga et al. for the second Gaussian. Dashed (dotted) curve represents contribution from the first (second) Gaussian term.

Fig. 3 χ^2 contours for fits to the subthreshold P data. Cross mark indicates value for σ_2 and A_2/A_1 extracted by Geaga et al. from data on backward proton production with the error bars quoted therein.

Fig. 4 $P + Cu \to \overline{P} + X$

Calculations containing coherent interactions with 2-nucleon and 3-nucleon clusters. Solid curve represents best fit. Dashed curve represents calculations containing parameterization of Vary and Pirner for the fraction of 6 quark and 9 quark bags in copper nucleus (with arbitrary normalization).

Table 1

E_p GeV	$P_{\bar{p}}$ GeV/c	data ($\bar{P}$) $d^2\sigma/dpd\Omega$ mb/sr-GeV/c	fit ($\bar{P}$)
6.1	1.37	$1.04 + 0.21 \times 10^{-2}$	1.16×10^{-2}
	1.20	$7.74 + 1.55 \times 10^{-3}$	8.32×10^{-3}
	0.97	$4.75 + 0.86 \times 10^{-3}$	4.32×10^{-3}
	0.87	$2.95 + 0.45 \times 10^{-3}$	2.76×10^{-3}
5.0	1.19	$1.89 + 1.18 \times 10^{-3}$	0.992×10^{-3}
4.55	1.37	$2.51 + 0.47 \times 10^{-4}$	2.84×10^{-4}
	1.20	$1.97 + 0.36 \times 10^{-4}$	2.65×10^{-4}
	0.97	$1.92 + 0.41 \times 10^{-4}$	1.74×10^{-4}
	0.87	$1.16 + 0.21 \times 10^{-4}$	1.10×10^{-4}
4.0	1.37	$2.91 + 0.73 \times 10^{-5}$	3.19×10^{-5}
	1.20	$5.0 + 1.0 \times 10^{-5}$	3.30×10^{-5}
	0.97	$3.31 + 0.72 \times 10^{-5}$	2.67×10^{-5}
	0.87	$3.1 + 0.77 \times 10^{-5}$	2.13×10^{-5}
3.5	0.97	$4.04 + 1.51 \times 10^{-6}$	2.26×10^{-6}
3.05	0.76	$8.28 + 3.68 \times 10^{-8}$	2.91×10^{-8}
2.88	0.76	$4.86 + 2.43 \times 10^{-8}$	6.51×10^{-9}

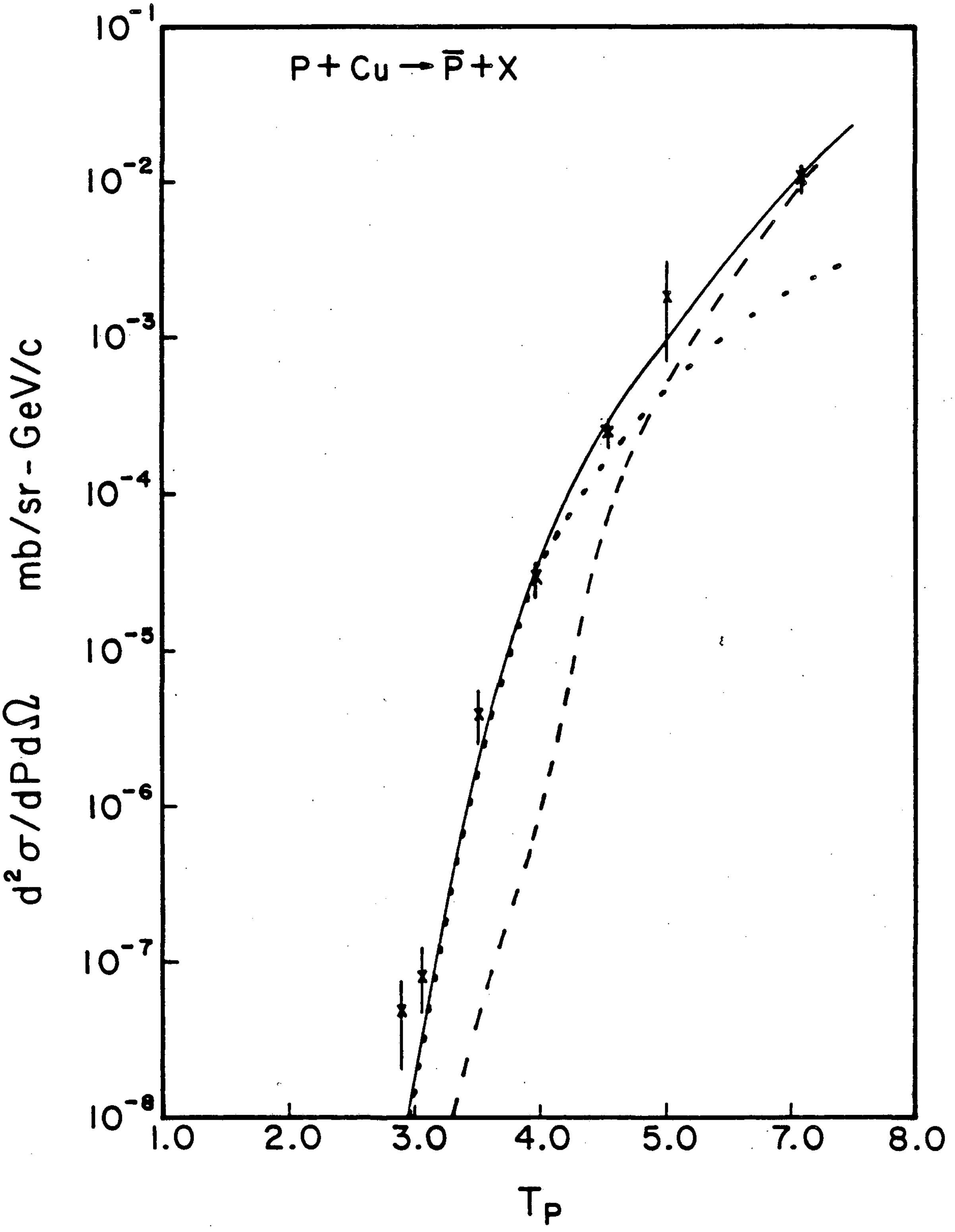

XBL 847-2862

figure 1

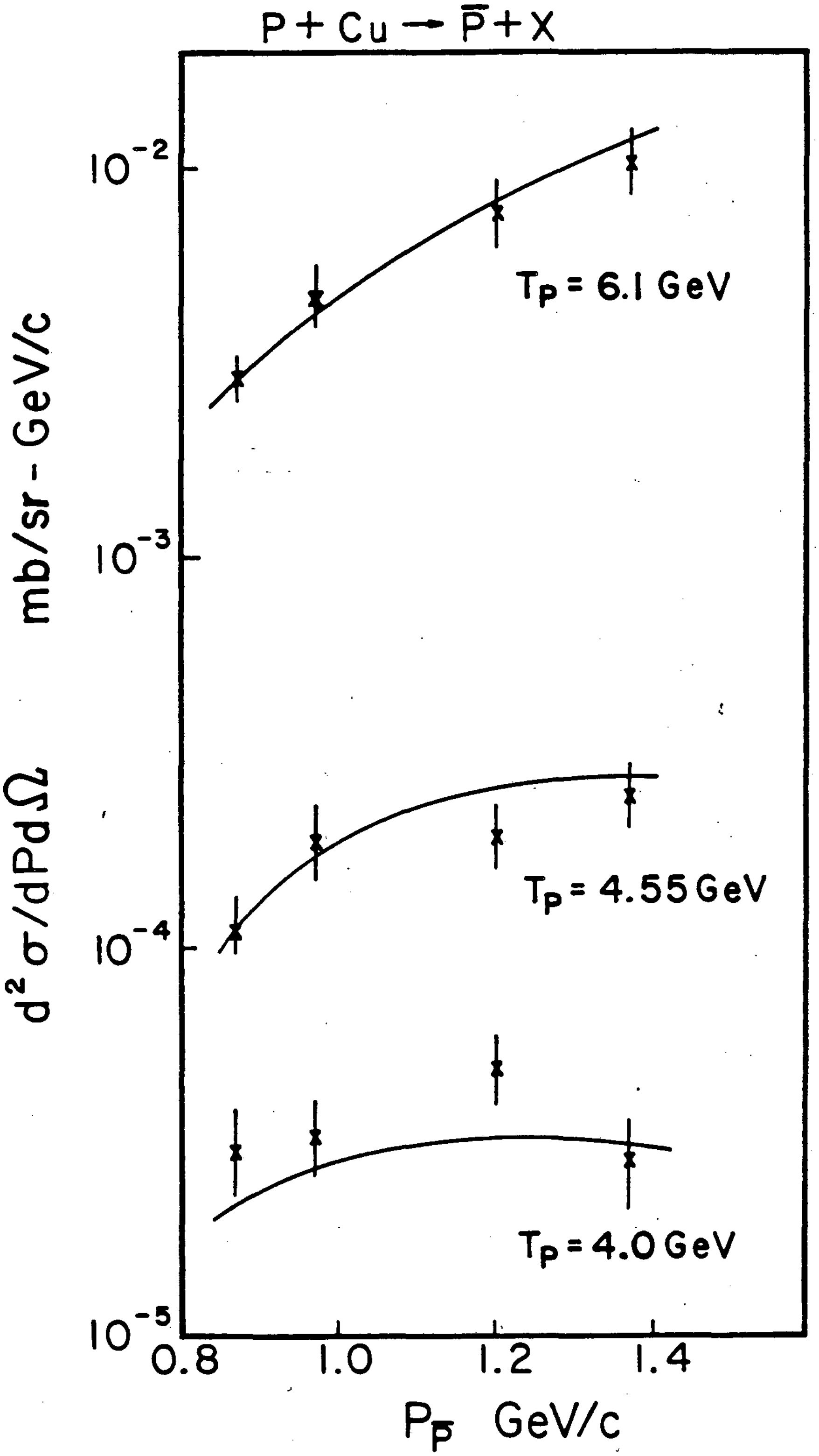

XBL 847-2863

figure 2

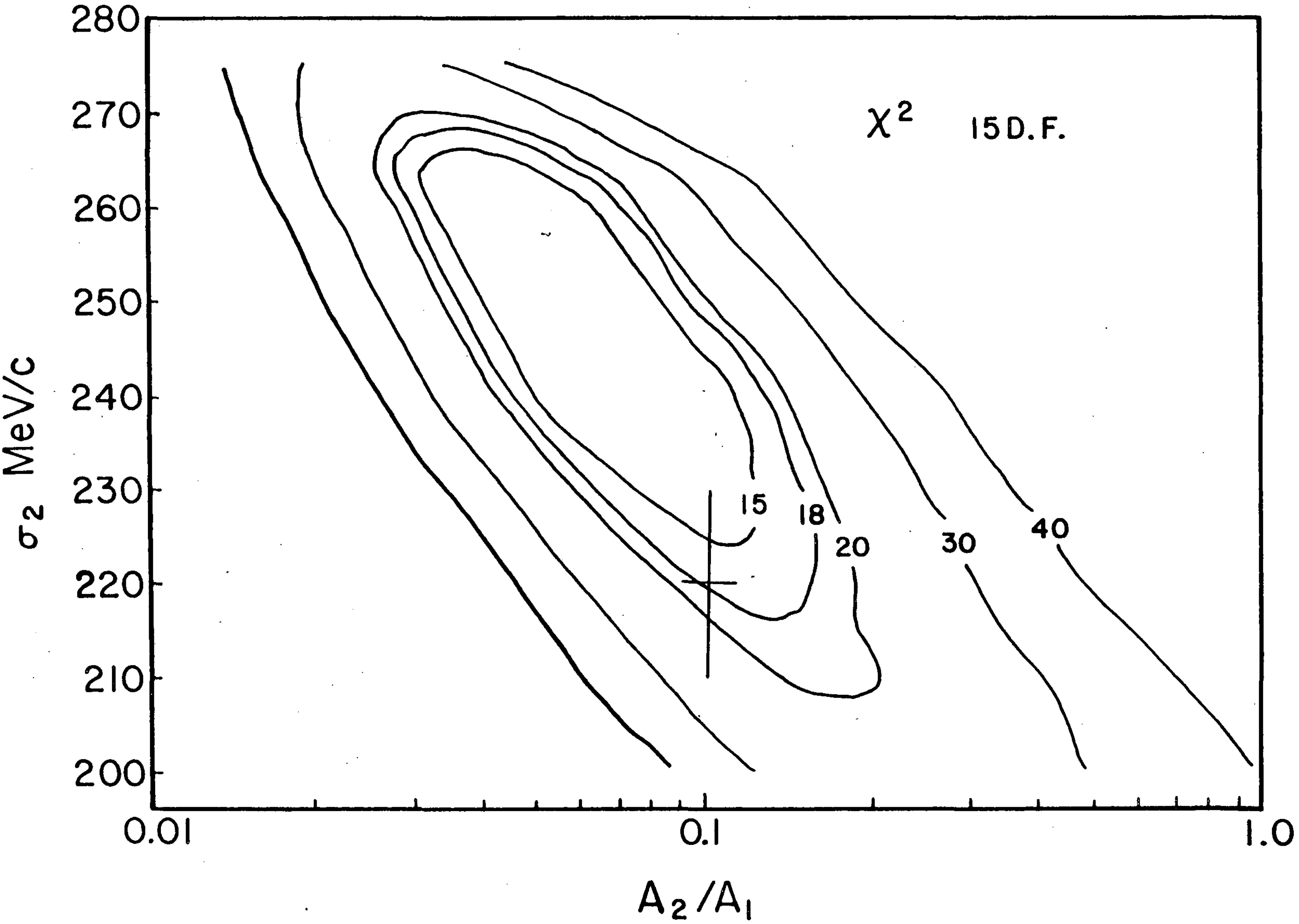

XBL 847-2864

figure 3

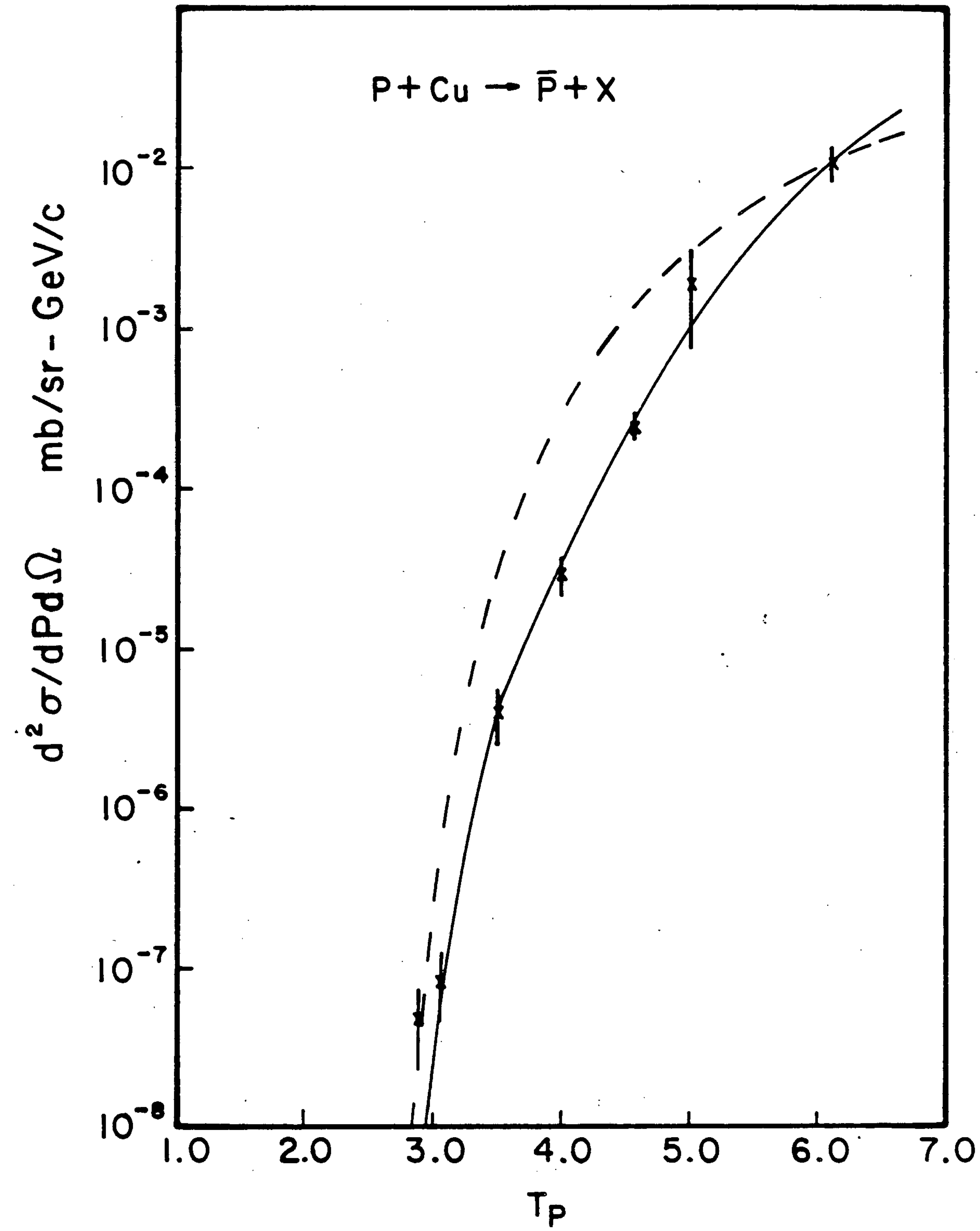

XBL 847-2861

figure 4

TECHNICAL INFORMATION DEPARTMENT
LAWRENCE BERKELEY LABORATORY
UNIVERSITY OF CALIFORNIA
BERKELEY, CALIFORNIA 94720